Catalysis Today 166 (2011) 47–52

Contents lists available at ScienceDirect

Catalysis Today

journal homepage: www.elsevier.com/locate/cattod

Catalytic behavior of Co/(Nanoβ-Zeolite) bifunctional catalysts for Fischer–Tropsch reactions

G. Espinosa[a,*], J.M. Domínguez[a], P. Morales-Pacheco[b], A. Tobon[a], M. Aguilar[a], J. Benítez[a]

[a] Instituto Mexicano del Petróleo, Programa de Ingeniería Molecular, Eje Central Lázaro Cárdenas Norte 152, Gustavo A. Madero, 07730 México, DF, Mexico
[b] Instituto Tecnológico Superior de Poza Rica, Depto. de Ingeniería en Nanotecnología, Luis Donaldo Colosio S.N., Col. Arroyo del Maíz, 93230 Poza Rica, Veracruz, Mexico

ARTICLE INFO

Article history:
Available online 15 February 2011

Keywords:
Beta zeolite
Bifunctional catalysts
Fischer Tropsch process

ABSTRACT

Cobalt supported on Beta zeolite catalysts were prepared by impregnation of metal salts in aqueous solution and were tested for the Fischer Tropsch reaction. The support consisted of a Beta zeolite composed by crystallites of nanometric dimensions and a SiO_2/Al_2O_3 molar ratio of about 50. This support was impregnated with $Co(NO_3)_2$ aqueous solution using different metal loads of 7.5, 10, 15 and 20 wt% Co. These materials were characterized by X-ray diffraction (XRD), high resolution transmission electron microscopy (HRTEM), N_2 adsorption (BET), thermal programmed reduction (TPR) and FTIR of adsorbed pyridine (i.e., surface acid sites distribution). All the catalysts showed a significant catalytic activity for the F–T reaction from synthesis gas ($CO + 2H_2$), in a continuous fixed bed reactor system. The catalysts presented a bifunctional character with a maximum of activity at a specific concentration of metal and particle size. In contrast, the selectivity patterns were strongly influenced by the support acid function, which promote the formation of isoparaffins from about 220 °C, which differ with most of conventional zeolites that show a relatively low activity for isomerization at this temperature, thus indicating an effect of the small Beta zeolite crystallites size over the catalytic activity of Co/Nanoβ-Zeolite.

Published by Elsevier B.V.

1. Introduction

The Fischer Tropsch (F–T) process is used today for the production of liquid fuels and useful chemicals [1–3] from a mix of synthesis gas ($CO + H_2$), in the presence of either supported or unsupported iron and cobalt metal catalysts [4–6]. As cobalt is less available than iron, many studies focused on preparing the F–T catalysts with a high dispersion of the Co phase over diverse metal oxides. For example, it was reported that F–T catalysts based upon Co supported on siliceous materials, produce high molecular weight linear chain paraffins and olefins, mainly [3]. Although the siliceous materials are considered relatively neutral as supports under F–T conditions, i.e., at temperatures between 190 and 260 °C, the Co based catalysts tend to produce isoparaffins [4]. These are considered secondary products and may be increased under conditions proper of integral reactors. However, the influence of the support acid function over the products distribution tends to enhance deviations with respect to a classical distribution. In particular, the surface acid function of zeolites is known to exhibit a selectivity towards lighter and branched products, even aromatics. Cobalt based catalysts supported on conventional zeolites like mordenite, ZSM5, Beta and Y zeolites have been reported to produce hydrocarbons in the middle chain range, which contrasts with the behavior of heavier cut obtained with silica supported cobalt catalysts [7–10]. Moreover, the mean crystallites size of zeolites seems a critical parameter for catalytic reactions in general, because smaller crystallites should present a greater proportion of surface active sites with respect to conventional zeolites, i.e., crystals of about 1 micron size [11,12]. Furthermore, crystallites of nanometric dimensions should present a shorter diffusion pathway for the reactant hydrocarbon molecules, which means short contact times or single contacts between reactants and active sites, which should lead to less coke formation. In order to explore these concepts and the influence of Beta support nanometric crystallites, a series of Co catalysts with distinct concentrations were prepared by impregnation and their catalytic behavior was tested under F–T conditions. In the literature there are no previous studies made on zeolitic materials of nanometric dimensions for F–T synthesis.

2. Experimental

2.1. Synthesis of support

The synthesis of Beta zeolite was carried out using aluminum powder (325 mesh, Baker) and fumed silica (0.007 μm, 390 m^2/g,

* Corresponding author.
E-mail addresses: gaespino@imp.mx (G. Espinosa), pmpachec@yahoo.com.mx (P. Morales-Pacheco).

0920-5861/$ – see front matter. Published by Elsevier B.V.
doi:10.1016/j.cattod.2011.01.025

Aldrich) as sources of aluminum and silicon, respectively. The template agent was a tetraethylammonium hydroxide solution (aqueous 35 wt%, from Aldrich). In the first place both aluminum and silicon sources were separately dissolved in the template solution, then were mixed and aged at room temperature with stirring during 4 h. The gel composition was 30 TEAOH:50 SiO_2:Al_2O_3:982 H_2O. This gel was aged in autoclave at 140 °C during 96 h. The materials thus obtained were washed in steps by centrifugation at 2500 rpm. Furthermore, the materials were dried overnight at 120 °C and were calcined at 550 °C for 6 h. The acid form of Beta was obtained by cationic exchange with 1 M solution of ammonium nitrate at room temperature, during 6 h. Furthermore, the materials were filtered, then washed thoroughly, dried and calcined at 550 °C for 6 h.

The cobalt was loaded on the Beta zeolite by impregnation with $Co(NO_3)_2$ aqueous solutions. The Co concentration in these solutions was calculated for obtaining 7.5, 10, 15 and 20 wt% Co on the dried catalysts. The impregnation was carried out at room temperature during 6 h, then was completely dried at 60 °C overnight and calcined at 300 °C during 3 h. The Co content was analyzed by Atomic Absorption Spectroscopy. The catalysts were labeled according to their Co nominal content, i.e., C7.5ZBN, C10ZBN, C15ZBN and C20ZBN.

2.2. Characterization

The X-ray diffraction patterns were recorded in a Siemens D-500 type diffractometer with CuKα radiation (λ_{Cu} = 0.154 nm) at 35 kV and 25 mA. The mean crystallite diameters of Co_3O_4 were calculated from the full width half-maximum (FWHM) of the most intense Co_3O_4 peak at $2\theta = 36.9°$ using Scherrer's equation. From the average size of cobalt oxide crystallites the mean diameter of cobalt metallic particles was estimated using the relationship $d_{Co(metal)} = 0.75 * d\ Co_{oxide}$ [13]. These values served to calculate the cobalt metal dispersion of the catalysts by means of the relationship $\%D = (96/d_{Co(metal)}$ [14,15]. A spherical geometry of the metal particles is assumed with a density of 14.6 at/nm^2.

Also, the structural features of the catalysts were characterized by means of high resolution transmission electron microscopy (HRTEM) using a JEOL (200 kV) 2200 FS microscope. The samples were mounted onto holey carbon coated copper grids after dehydration treatment overnight at 200 °C.

The surface area of some materials and other textural properties were determined by nitrogen adsorption/desorption using a Micromeritics ASAP 2405 apparatus. The samples were outgassed at 350 °C under vacuum, overnight.

The Bronsted and Lewis surface acidity distribution was monitored by means of pyridine adsorption using Fourier transform infrared spectroscopy (FTIR) in a spectrometer Nicolet, Model 710. Self-supported wafers were prepared from powder samples and these were mounted on a pyrex cell fitted with CaF_2 windows. The Co catalysts were first reduced for 1 h at 400 °C, under hydrogen flow, before obtaining the IR spectra. The system was purged under vacuum while the temperature was decreased to 25 °C. Then, pyridine was adsorbed for 30 min under pressure of 20 torr. FTIR spectra were recorded progressively after outgassing at 100, 200, 300 and 400 °C.

The TPR profiles corresponding to the catalysts based upon Co/Beta zeolite were obtained in a Altamira Instruments II apparatus, where the powder samples were first dried at 200 °C during 1 h, then the temperature was lowered down to room temperature and the reduction was performed under H_2 (10 vol% in Argon) using a heating ramp of 5 °C/min, until 850 °C.

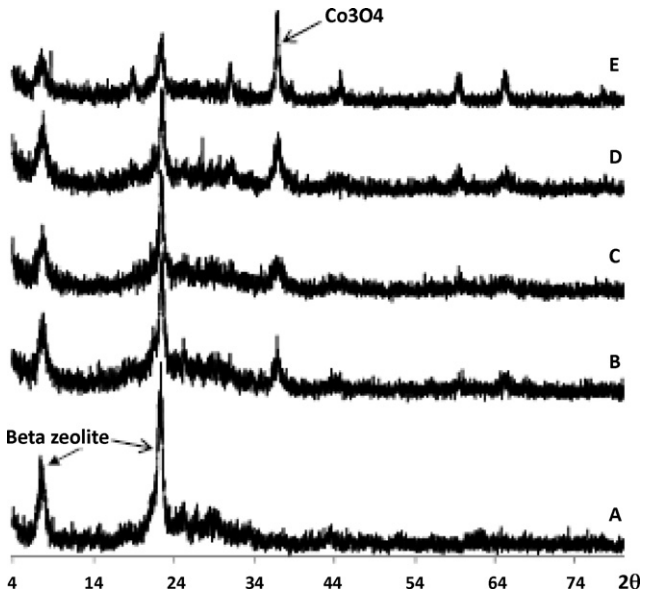

Fig. 1. XRD patterns from catalysts of Co supported on Beta zeolite. (A) ZBN pure Beta zeolite, (B) C7.5ZBN, (C) C10ZBN, (D) C15ZBN, and (E) C20ZBN.

2.3. Catalytic tests

The catalytic tests were carried out in a stainless steel fixed bed type reactor system which was fitted with automated controls for pressure, temperature and volumetric fluxes. For each run 1 g of the catalyst was activated in situ under H_2 flow at 400 °C, atmospheric pressure, during 6 h. The F–T reactions conditions were the following: pressure of 1 MPa, molar ratio $H_2/CO = 2$; $(CO + H_2)$ gas flow: 3.6 l/h at 220 °C. The synthesis gas contained 5% N_2 as an internal standard to determine the carbon monoxide conversion. The effluent gases were monitored every 6 h on-line, using a Varian STAR 3600CX Chromatograph fitted with a 60 m H-P Plot column and a TCD detector, which allowed the analysis of CO, H_2, N_2, CO_2 and C_1–C_6 (gaseous). The condensable products were collected in a cold trap that was kept at the same pressure than the reactor. The conversion is obtained by averaging the reactants disappearance in function of the time on stream (i.e., 24 h). The accumulated products were analyzed off-line by gas chromatography and mass spectrometry.

3. Results

Table 1 summarizes the properties of both cobalt catalysts and supports. The Co content was determined by atomic absorption spectrometry, which showed compositional values slightly lower than the nominal ones.

3.1. Structural features

Fig. 1 shows the XRD patterns of the catalysts and the Beta zeolite support. In general, these patterns contain two peaks that are typical of Beta zeolite, i.e., a peak at 8° (2θ) and the more intense peak at 23° (2θ). The mean size of the cobalt oxide crystallites was determined using Scherrer's equation and the dispersion percentage of metallic cobalt was estimated and reported in Table 1. The average size of cobalt oxide crystallites was in the 7–28 nm range. The catalyst with 7.3 wt% Co, i.e., C7.5ZBN, contains a mean size of 16 nm, which is larger than those calculated for the catalysts containing 9.6 wt% (i.e., 7 nm) and 13.5 wt% (i.e., 9 nm) Co, which suggests that the lower content of cobalt is not decisive for obtaining a good metal dispersion.

Table 1
Properties of Co catalysts supported on nanometric Beta zeolite.

Catalysts	Co (wt%)	Langmuir surface area (m^2/g)	Pore volume (cm^3/g)	Co_3O_4 crystallites mean size (nm)	Co metal dispersion %	Reduction[a] %	Bronsted acid sites[b] (μmol/g)
ZBN	–	747	0.42	–	–	–	64
C7.5ZBN	7.3	595	0.35	16	8	48	72
C10ZBN	9.6	553	0.32	7	18	77	47
C15ZBN	13.5	538	0.31	9	14	79	26
C20ZBN	18.5	492	0.29	28	5	59	55

[a] Obtained from the TPR experiments.
[b] The amount of Bronsted acid sites is calculated at 200 °C.

On the other hand, there is a diminution of the XRD peaks intensities of Beta with increasing Co content, i.e., the catalyst C20ZBN (i.e., with a real Co content of 18.5 wt%), presents a strong diminution of the zeolite XRD peaks intensity, but the peaks of the Co_3O_4 phase become more important, thus suggesting that the cobalt oxide crystallites are larger as the cobalt content increases. In turn, the largest Co oxide particles might screen some XRD reflections arising from the nanometric Beta zeolite crystallites.

The study by HRTEM (Fig. 2A–C) shows that Beta crystallites have a diameter of about 5–20 nm (i.e., a comparison can be made with the 20 nm bar situated at the bottom of the images), thus showing the presence of crystallites agglomerates that are confirmed by the presence of Moiré type fringes; these fringes are the result of electron beam interference occurring by multiple scattering from the superimposed crystals, which change of direction around the particles. In some areas of Fig. 2A and B one observes the pore arrangement that is characteristic of Beta zeolite, which changes from black to white due to local thickness variations and crystallites tilting. Also, the small dark areas correspond to the more dense cobalt oxide particles and these areas grow with the cobalt concentration, thus suggesting that Co is concentrated rather than dispersed evenly on the support. These results are in agreement with the X-ray diffraction peaks of cobalt oxide and the average sizes calculated from these data. The dispersion values follow the expected correlation (Table 1). A low metallic dispersion of Co has been reported elsewhere [8,9] but it has been claimed [16] that the cobalt dispersion depends of several factors, apart the impregnation step, i.e., the calcination temperature. In this work the calcination temperature was set at 300 °C, which is relatively low, in order to minimize the migration of cobalt species during the decomposition step. However, the results showed a rather poor metallic dispersion while the

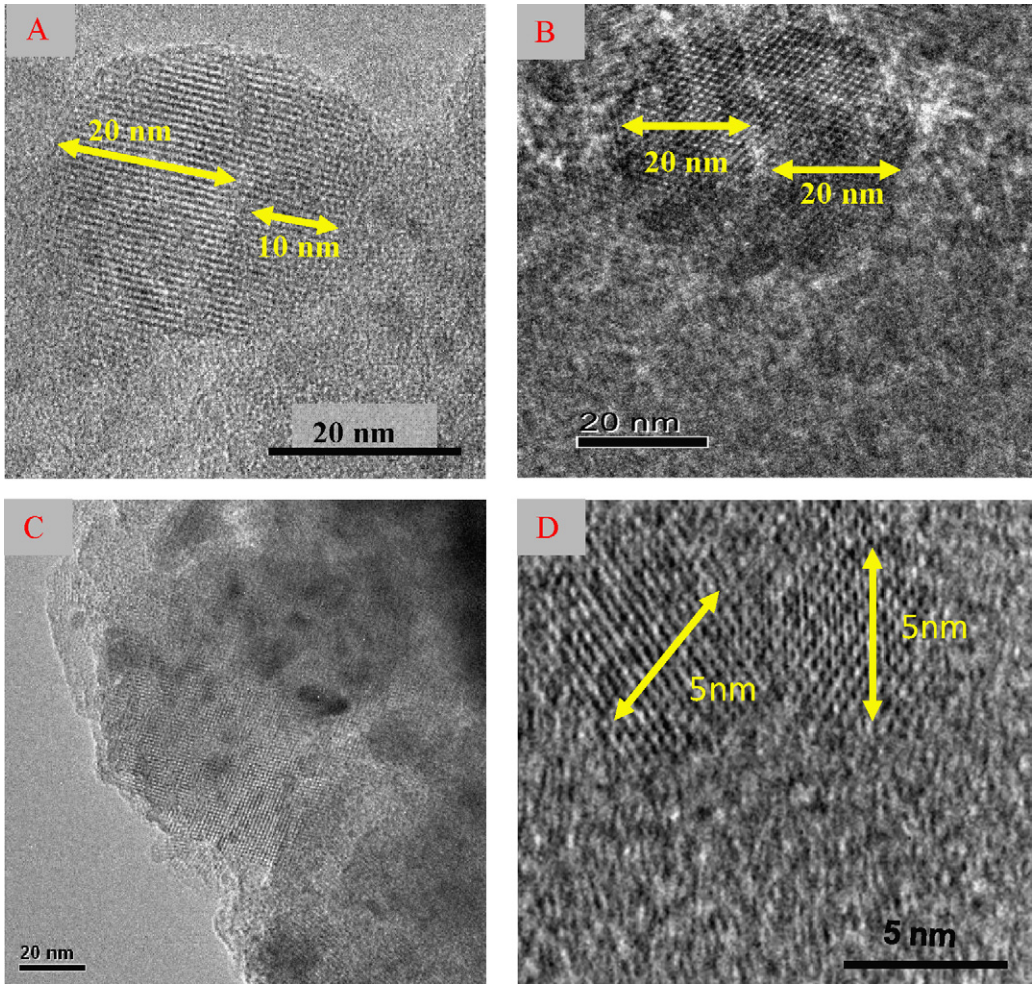

Fig. 2. Beta crystallites with diameter of about 5–20 nm.

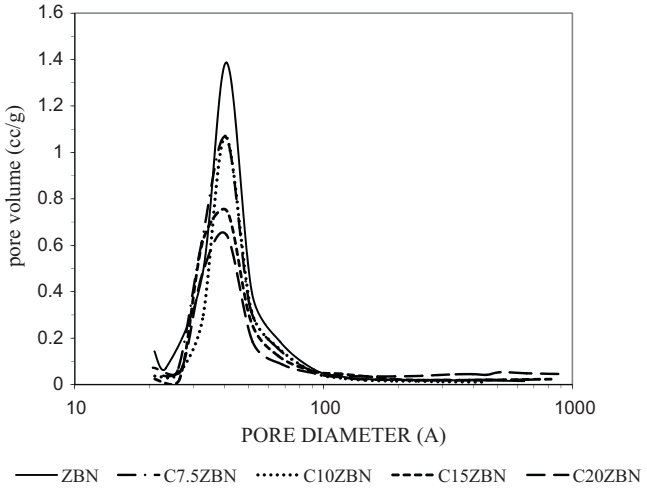

Fig. 3. Pore diameters distribution of the nanometric Beta zeolite and catalysts.

catalysts consisted of a mix of cobalt oxide particles of different sizes.

3.2. Textural properties

Fig. 3 shows the pore volume distribution from nitrogen desorption experiments (BJH's method). Mainly, a monomodal distribution is centered around 3 nm (see Table 1), which more probably arises from voids between the aggregates of crystallites. Also Fig. 3 shows the progressive diminution of the monomodal peak as well as the surface area in function of the Co concentration (Table 1) in the metal supported catalysts, which may indicate that the cobalt oxide phase could be located into the voids left by the crystalline aggregates. This result coincides with the fact that the mean size of cobalt oxide crystallites is much larger than the pore opening of Beta zeolite channels (0.57 nm × 0.75 nm), as revealed by TEM; thus, the cobalt oxide crystallites are more probably located out the pore network of the Beta zeolite crystallites.

3.3. Surface acidity

Fig. 4 illustrates the FTIR spectra after out-gassing the samples at 200 °C, which is the temperature nearest to the reaction temperature set for the catalytic reaction. As mentioned in Section 2.2, the catalysts were pretreated with hydrogen at 400 °C (except ZBN),

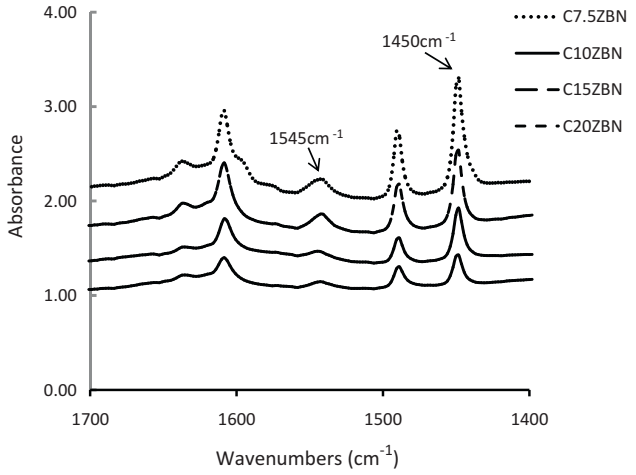

Fig. 4. FTIR spectra of catalysts obtained from adsorbed Pyridine at 200 °C.

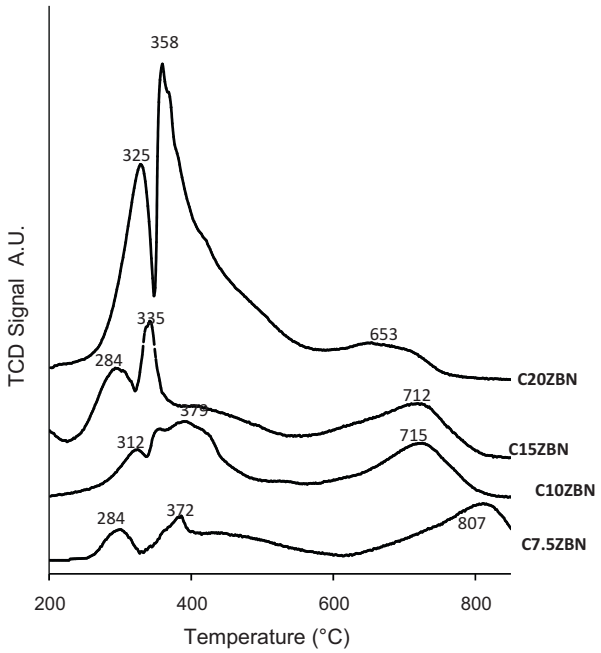

Fig. 5. TPR profiles of Co supported on Beta nanometric crystallites.

previous to the measurements of pyridine adsorption, with the purpose of having temperatures close to the catalytic tests conditions. The IR spectra displayed clearly the vibrations arising from Bronsted acid type sites at 1545 cm^{-1}, which correspond to Lewis type acid sites at 1450 cm^{-1}. It is observed that C7.5ZBN and C20ZBN catalysts present a band at 1545 cm^{-1}, which is higher than C10ZBN and C15ZBN. It was found that C10ZBN and C15ZBN contain a minor amount of Bronsted acid sites and the corresponding values are reported in Table 1. However, there is no a clear trend related to the cobalt concentration, but the cobalt particles size may have an influence on the surface acidity. The catalysts containing a high proportion of large particles, i.e., C7.5ZBN and C20ZBN (Table 1), seem to show a weak interaction with the Beta zeolite and, after the reduction treatment, the catalysts keep their surface acid sites (Fig. 5).

3.4. TPR experiments

The reduction percentage of the catalysts in the 200–850 °C range was determined from the relationship between consumed hydrogen and theoretical values corresponding to a stoichiometric factor. The total reduction of cobalt should occur for a hydrogen to cobalt ratio of 1.5. For this, the Co content was determined by atomic absorption spectroscopy. The results are reported in Table 1 while Fig. 5 displays the TPR profiles of the catalysts series, where one observes four peaks corresponding to the transitions of Co_3O_4. The first one is assigned to the reduction of the Co^{3+} phase to Co^{2+} at about 284 °C for the C7.5ZBN and C15ZBN catalysts, while C10ZBN and C20ZBN show this reduction peak at about 325 °C. The latter may be assigned to reduction of large particles of cobalt oxide [16]. The second peak occurs at a higher temperature and should correspond to the transition $Co^{2+} \rightarrow Co^0$, which combines the reduction of any Co^{2+} phase remaining in the initial Co_3O_4 phase plus the fraction of Co^{2+} initially formed in the first reduction step. However, the second and third peak overlap and extend over a wide temperature range, thus suggesting several interactions occurring between the cobalt species and the surface of nanometric zeolite crystallites.

Table 2
Catalytic activity and product distribution.

Catalyst	Conversion (%)	CO_2 (wt%)	C_1 (wt%)	C_2–C_5 (wt%)	C_6–C_{20} (wt%)
C7.5ZBN	20.5	38.2	38.9	14.8	7.9
C10ZBN	21	0	41	43.9	14.9
C15ZBN	30.2	7.4	33.3	33	26.2
C20ZBN	13	0	36.1	44.6	19.3

$T = 220\,^{\circ}C$; $P = 10\,kg/cm^2$, H_2/CO molar ratio = 2.

Also, it is reasonable to assume that small cobalt moieties interact with the zeolite surface through the more extended contact surface in between, which might lead to substitution of some surface support protons by Co^{2+} ionic species, i.e., a ionic exchange between H^+ (linked to zeolite) and Co^{2+} cations, regardless of the impregnation method used. The possible role of cationic cobalt for counterbalancing the zeolite surface charge is demonstrated neither by XRD nor by HRTEM methods, but if the ionic cobalt exchange occurs on both external and internal zeolite pore walls that contain the acid sites, it is possible that the reduction requires higher temperatures. In addition, it was reported elsewhere that metal oxide species require higher temperatures for reduction [17]. Thus, it is probable that after activation at 400 °C still remain some of the cobalt species that are not in a metallic state, which do not contribute to the catalytic properties in the F–T reactions.

3.5. Catalytic tests

Table 2 summarizes the results obtained on the conversion of synthesis gas over the supported metal (Co) catalysts, as well as the products distribution. These results are based on the mass balance of the feed and products as a percentage of the weight of carbon converted. These catalysts present a relatively low activity for the Fischer–Tropsch reaction, with an overall carbon monoxide conversion between 13 and 30%, which is similar to the activity reported previously for conventional zeolite supported Co catalysts [9,10].

The CO conversion on the C15ZBN catalysts passes for a maximum and the formation of C_5–C_{14} products follow this trend too, while the highest conversion rates and yield seem dependent on the content of Co. Also, the CO_2 forms as a byproduct but it is not clear its relationship with respect to the cobalt content. This product is relatively unusual when using Co based catalysts, because the water is the main byproduct, which arises from the lower ability of Co for promoting the water gas shift (WGS) reaction. The yield of liquid products (C_{5+}) is relatively low but heavier liquid hydrocarbon and waxes were not detected. The selectivity pattern is different for each catalyst, however, there is a trend in all the cases towards the production of isoparaffins. As mentioned above, despite the low reaction temperature, i.e., at 220 °C, the formation of aromatics occurs. A high GHSV of about 1800 h^{-1} was used in order to minimize secondary reactions. It is known that Co starts to be active at about 190 °C, but the zeolites usually require activation temperatures between 240 and 260 °C for effecting the catalytic isomerization of light paraffins [18]. In contrast to this, the F–T reactions favor the formation of light products [19] with increasing temperature, i.e., until 260 °C.

4. Discussion

Liquid hydrocarbons were obtained by means of the Fischer–Tropsch process form catalytic conversion of synthesis gas ($CO + H_2$) with a H_2/CO ratio of 2, where the catalysts seem to follow a similar profile, that is the appearance of a maximum for carbon numbers C_9–C_{10}, as shown in Fig. 6, which indicates the zeolite contribution to selectivity. However, the products distribution presents several differences in function of the Co content. The C10ZBN and C15ZBN catalysts are similar to each other but some differences appear with respect to the other catalysts, which present a higher proportion of olefins with respect to *n*-paraffins, In this case some diffusion effects are discarded because all the catalysts have practically the same textural properties, while the gas flow is relatively high. Usually, the hydrogenation reaction in the F–T process is a termination step because the hydrocarbons chain growth is more probably carried out by α-olefins reinsertion [19,22].

On the other hand, the catalysts C10ZBN and C15ZBN contain the lower crystallite size, as estimated from Scherrer's method. This may contribute to a strong interaction between small metal particles and the support surface, which might account for some deviation of the properties of small metal particles with respect to the bulk [20,21]. It has been claimed that the active phase in the catalytic conversion of synthesis gas is the fully reduced state of the Co phase [5,23] and, for the present case, it is worth mentioning that the C15ZBN catalyst has a reduction percentage higher than the rest of the catalysts, as determined by TPR; in parallel, this catalyst is more active for the conversion reaction. Moreover, its relatively high metallic dispersion contributes to increase the number of active metal sites. In fact, the presence of unreduced Co^{2+} was evaluated indirectly by FTIR of adsorbed Pyridine, i.e., coincidently these two catalysts, C10ZBN and C15ZBN, contain the lower amount of acid sites at 200 °C, which indicates that a portion of cobalt remains as Co^{2+}, which in turn might occupy the proton sites. Another result supports this hypothesis: the lower formation of isoparaffins that was detected in the liquid products corresponds to those catalysts (Table 3, Fig. 6). In contrast to this, the C7.5ZBN and C20ZBN catalysts produce about 40% of isoparaffins, which is in agreement with the presence of a more prominent acid function. Also, the evidence showed that the samples were very heterogeneous, for example the surface acidity of C20ZBN does not fit a linear model based upon the progressive suppression of surface acidity with the Co concentration.

In summary, the activity of the cobalt based catalysts for F–T synthesis depends in the first place on the amount of metallic sites available for the formation of hydrocarbon chains but in presence of the acid function the linear chains evolve to more branched and lighter hydrocarbon molecules. These results suggest two trends: one is represented by the couple C10ZBN and C15ZBN, while the other is represented by C7.5ZBN and C20ZBN catalysts. The former couple is composed by catalysts that have smaller cobalt oxide particles, with these particles being in a reduced state that present a higher amount of surface metallic sites, thus correlating well with their conversion levels. Some cobalt species should interact strongly with the external surface sites of the nanometric Beta zeo-

Table 3
Product distribution of the liquid phase.

Catalysts	C7.5ZBN	C10ZBN	C15ZBN	C20ZBN
Aromatics	11.8	7.2	13.2	8.81
Iso-paraffins	40.6	26.7	32	42
Naphthenes	1.6	1.04	1.7	0.64
Olefins	19.7	45.7	33	11
Oxygenates	1.4	2.4	1.7	1.2
Paraffins	25	17	18.5	36.7

Products collected after 24 h on stream.

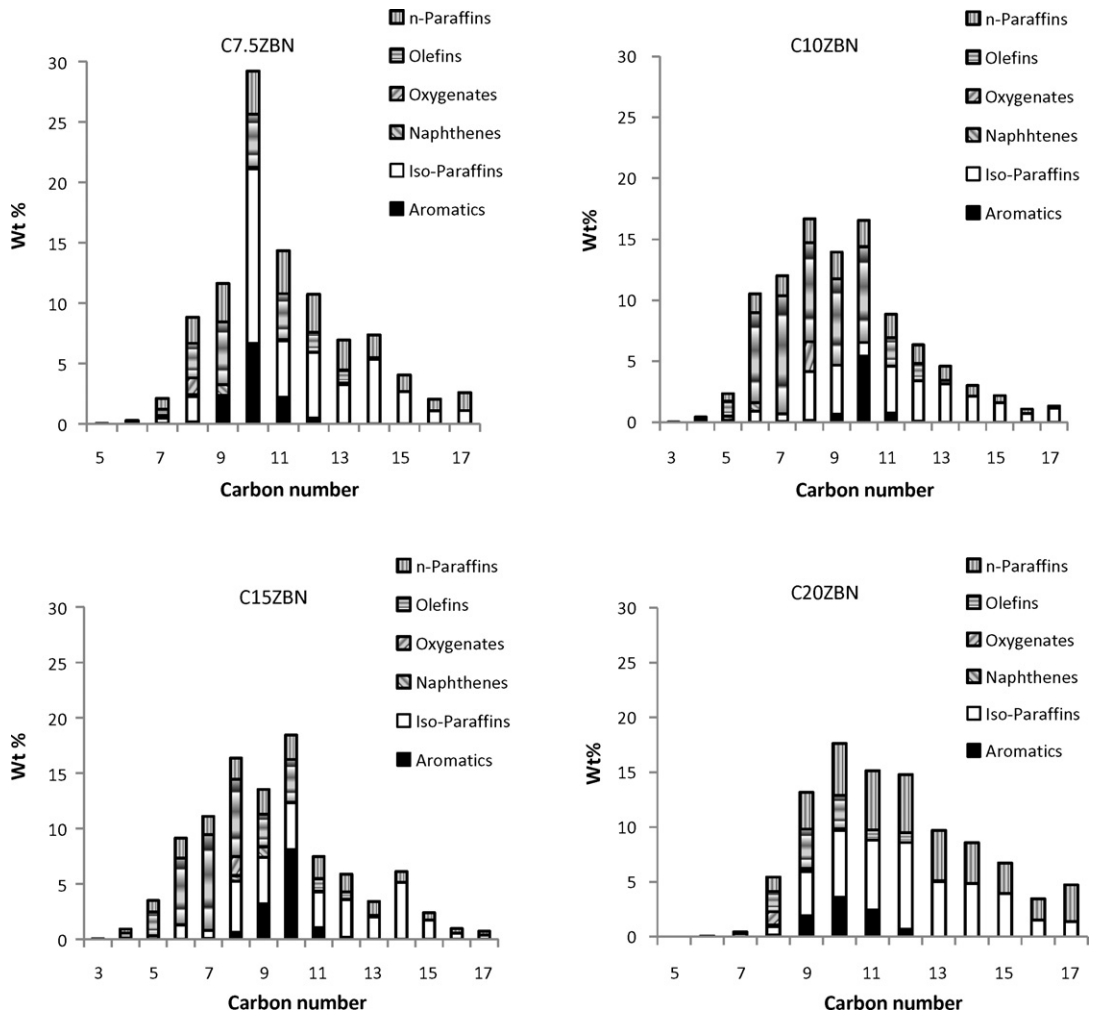

Fig. 6. Hydrocarbons distribution of the liquid product after 24 h of TOS.

lite, thus causing a partial poisoning effect of the acid function, which in turn produces a minor proportion of isoparaffins formation. The C7.5ZBN and C20ZBN catalysts contain relatively large metal particles, which means a minor amount of surface metallic sites available for catalytic F–T reactions, even for the catalyst having the higher content of Co, i.e., C20ZBN. Thus, the conversion is lower than the previous cases, but the acid sites are relatively "free" of promoting the catalytic isomerization reactions, as it is deduced from the selectivity patterns and Bronsted type acid sites, which are obtained by FTIR/pyridine adsorption.

5. Conclusions

The catalysts based upon supported cobalt on nanometric Beta zeolite are active in F–T reactions and their behavior seems bifunctional, that is the metal particles and the surface acidic function of the support play a combined role in the synthesis gas conversion and isomerization reactions, respectively. The selectivity is strongly oriented to isoparaffins at a temperature equal to or above 220 °C. The catalytic behavior for the F–T reactions depends on the size of the cobalt metal particles, i.e., the number of metal sites available. The acid function interacts strongly with the small metal particles and this interaction may affect the acid catalytic functions mainly.

References

[1] H. Schulz, Appl. Catal. A: General 186 (1999) 3–12.
[2] A.C. Vosloo, Fuel Process. Technol. 71 (2001) 149–155.
[3] H. Pichler, Advances in Catalysis, vol. IV, Academic Press, New York, 1952, p. 271.
[4] R.L. Espinoza, A.P. Steynberg, B. Jager, A.C. Vosloo, Appl. Catal. A: General 186 (1999) 13–26.
[5] E. Iglesia, Appl. Catal. A: General 161 (1997) 59–78.
[6] A. Tavasoli, R.M. Malek Abbaslou, M. Trepanier, A.K. Dalai, Appl. Catal. A: General 345 (2008) 134–142.
[7] B. Ernst, S. Libs, P. Chaumette, A. Kiennemann, Appl. Catal. A: General 186 (1999) 145–168.
[8] C. Ngamcharussrivichai, X. Liu, X. Li, T. Tharapong Vitidsant, K. Fujimoto, Fuel 86 (2007) 50–59.
[9] Y. Li, T. Wang, C. Wu, Y. Lv, N. Tsubaki, Energy Fuel. 22 (2008) 1897–1901.
[10] S. Bessel, Appl. Catal. A: General 126 (1995) 235–244.
[11] F. Vaudry, F. Di Renzo, F. Fajula, P. Schulz, J. Chem. Soc.: Faraday Trans. 94 (4) (1998) 617.
[12] D. Barthomeuf, Mater. Chem. Phys. 17 (1987) 49.
[13] D. Schanke, S. Vada, E.A. Biekkan, A.M. Hilmen, A. Hoff, A. Holmen, J. Catal. 156 (1995) 85.
[14] R.C. Reuel, C.H. Bartholomew, J. Catal. 85 (1984) 63.
[15] R.D. Jones, C.H. Bartholomew, Appl. Catal. 39 (1988) 77.
[16] A. Martínez, J. Rollan, M.A. Arribas, H.S. Cerqueira, A.F. Costa, E.S.A. Falabella, J. Catal. 249 (2007) 162–173.
[17] E. van Steen, G.S. Sewell, R.A. Makhothe, C. Micklethwaite, H. Manstein, M. de Lange, C.T. O'Connor, J. Catal. 162 (1996) 220.
[18] H. YueChu, M.P. Rosynek, J.H. Lundsford, J. Catal. 178 (1998) 352.
[19] E.W. Kuipers, C. Scheper, J.H. Wilson, I.H. Vinkenburg, H. Oosterbeek, J. Catal. 158 (1996) 288–300.
[20] L. Guczi, I. Kiricsi, Appl. Catal. A: General 186 (1999) 375–394; E. Kikuchi, R. Sorita, H. Takahashi, T. Matsuda, Appl. Catal. A: General 186 (1999) 121–128.
[21] A.Y. Khodakov, Catal. Today 144 (2009) 251–257.
[22] H. Schulz, M. Claeys, Appl. Catal. A: General 186 (1999) 71–90.
[23] Y. Ji, Z. Zhao, A. Duan, G. Jiang, J. Liu, J. Phys. Chem. C 113 (2009) 7186–7199.